Experimental and Numerical Studies on the Performances of Stone Column and Sand Compaction Pile Reinforced Hong Kong Marine Clay

by

Wei-Qiang FENG (Postdoctoral Fellow)

Department of Civil and Environmental Engineering,

The Hong Kong Polytechnic University, Hung Hom, Kowloon, Hong Kong. China

Email: fengweiqiang2015@gmail.com

Dao-Yuan TAN (Postdoctoral Fellow, Corresponding Author)

Department of Civil and Environmental Engineering

The Hong Kong Polytechnic University, Hung Hom, Kowloon, Hong Kong, China

Email: rztdy2009@gmail.com

Jian-Hua YIN (Chair Professor)

Department of Civil and Environmental Engineering

The Hong Kong Polytechnic University, Hung Hom, Kowloon, Hong Kong, China

Tel: (852) 2766-6065, Fax: (852) 2334-6389, Email: cejhyin@polyu.edu.hk

Jie-Qiong QIN (Ph.D. candidate)

Department of Civil and Environmental Engineering

The Hong Kong Polytechnic University, Hung Hom, Kowloon, Hong Kong, China

Email: jieqiong.qin@connect.polyu.hk

and **Wen-Bo CHEN** (Postdoctoral Fellow)

Department of Civil and Environmental Engineering

The Hong Kong Polytechnic University, Hung Hom, Kowloon, Hong Kong, China

Email: geocwb@gmail.com

Manuscript submitted to *International Journal of Geomechanics* for possible publication as a Technical Note

Nov. 2019

Abstract: Stone columns (SCs) and sand compaction piles (SCPs) are widely utilized as effective methods to increase the bearing capacity and reduce the settlement of soft ground. In this study, a physical model test was conducted to compare the performances of the SC and SCP improved Hong Kong Marine Clay (HKMC) grounds. The finite element (FE) modelling was performed to analyze the settlement and stress increment. A practical equation related to the area replacement ratio and the friction angle of columns is proposed for determining the creep improvement ratio of soft ground treated by columns, which agrees well with the creep improvement ratios from the FE simulations.

Keywords: sand compaction pile; stone column; marine clay; creep improvement ratio

Introduction

Ground columns have been widely used in the improvement of soft soils to increase the bearing capacity, reduce total and differential settlements, accelerate consolidation and mitigate liquefaction. Stone Columns (SCs) and Sand Compaction Piles (SCPs) are two of the most widely applied column-based ground improvement techniques (Han and Ye, 2001; Kitazumi, 2005). Recently, SCs and SCPs have been widely utilized in Hong Kong Marine Clay (HKMC) to support seawalls in the artificial island for Hong Kong Boundary Crossing Facilities (HKBCF). SC and SCP play the roles of densification, reinforcement, and drainage related to the incorporated material (Bouassida and Carter, 2014). The stiffness of the columns is normally higher than that of the surrounding soft soil, larger stress concentrates on the columns with the assumption of equal strain. Stress concentration ratio (*n*-value) is defined as the ratio of the vertical stress acting on the column to that on the surrounding soil (Poorooshasb and Meyerhof, 1997):

$$n = \frac{\Delta\sigma_c}{\Delta\sigma_s} \tag{1}$$

where $\Delta\sigma_c$ and $\Delta\sigma_s$ are the stress increments on the column and the surrounding soil when the vertical loading is applied on the improved ground. However, there is a lack of direct comparison between the SC and SCP treated soft grounds in a drained boundary condition.

The creep behavior widely exists in soft soils and directly related to long-term settlement (Yin *et al.,* 2011). For HKMC, stress-strain-strength behavior is well studied by many researchers. The viscous behavior including creep and the strain-rate dependent behavior should be considered for this type of soft soil (Feng *et al.,* 2017). Pugh (2016) reported that the ignorance on the creep of soft soil resulted in two serviceability failures of the SC treated very soft ground in real projects. Therefore, the time-dependent behavior of the composite foundation formed by SC/SCP columns and HKMC is also necessary to be considered.

The settlement improvement factor, β, is utilized to describe the influence of area replacement ratio on the total settlement of the composite foundation (Sexton *et al.*, 2017):

$$\beta = \frac{S_{untreated}}{S_{treated}}\bigg|_{t=36500day} \quad (2)$$

where $S_{untreated}$ and $S_{treated}$ are the total settlements of untreated and column treated soft soil ground subjected to the same applied load for t=36500 day, respectively. A similar parameter $\beta_{consolidation}$ is defined as the consolidation settlement improvement factor for the soft soil with no creep. Similarly, the creep improvement ratio β_{creep} is defined as the creep coefficient of untreated ground and that of treated ground.

This study is to compare the performances of the SC and SCP in improving the strength and reducing the settlement of the HKMC soft ground and to investigate the effects of ground columns on the long-term performance of the column improved ground. A physical modelling experiment on the response of the SC and SCP treated soft ground subjected to external footing loads was conducted. An FE modelling was performed to examine the influences of the area replacement ratio, friction angle, and Young's modulus on the creep behavior of the ground improved by columns (specified on SCs and SCPs).

Physical Model Test and Procedures

Basic Properties of Clay and Column Materials and Preparation

The HKMC was taken from the site of the artificial island for HKBCF in Hong Kong. The plastic limit and liquid limit of the HKMC are 24.6% and 52.7%, respectively. The specific gravity, G_s, of HKMC is 2.56. HKMC belongs to the MH based on the Unconfined Soil Classification System (USCS). According to BSI (2016), the maximum and minimum dry densities are 1620 kg/m^3 and 1425 kg/m^3 for the standard sand material, 1480 kg/m^3 and 1200 kg/m^3 for the aggregate material. The aggregate is clarified as silty gravel with sand (group symbol is GM) with the coefficient of curvature of 0.98 and the coefficient of uniformity of 2.59; the standard sand belongs to clayey sand (group symbol is SC) with the coefficient of curvature of 0.568 and the coefficient of uniformity of 4.12.

A steel box with inner dimensions of 1000mm×600 mm×800 mm was used as the container for the physical model test, as shown in Figure 1. Lubricating grease was spread on the inner surfaces of the steel box and a plastic film was attached to the inner surface of the steel tank. First, the HKMC was mixed with water to prepare a fully saturated slurry with the moisture content about 1.9 times of liquid limit. A pre-consolidation pressure of 10 kPa was applied on the surface of the HKMC by dead weights. After the pre-consolidation stage, an SC and an SCP were installed into the HKMC for comparison under the same loading condition. The arrangements of the two columns and transducers are shown in Figure 1. Earth pressure cells and pore water pressure transducers were utilized and installed in the physical model. The capacity of pore-water pressure transducers is 1 MPa with an accuracy of 1 kPa in this study. Earth pressure cells (TML model KDA-PA/KD-A) were calibrated with a capacity of 1000 kPa (Zhou et al. 2011). After the installation of the SC and SCP, a sheet of geotextile covered by a 50 mm thick sand layer was placed on the surface of HKMC. A plywood plate with a thickness of 15 mm was placed above the sand layer to provide the equal-strain condition, as shown in Figure 1(b). The uniform vertical loading of 40 kPa was imposed by a water-pressurized rubber membrane underneath a bolt-fixed steel cap. The detail of this membrane has been described in Yin and Su (2006).

Procedure Description

First, the vertical pressure of 40 kPa was applied by the GDS pressure/volume controller for three days under the drained condition. The stress changes on the top of the SC and the SCP and at the top surface of the HKMC were monitored. The dissipation of the excess pore water pressure in the HKMC was also monitored during the testing progress. Then, an undrained load test was conducted using a hydraulic jack to investigate the load-settlement relationship of the SC and SCP. The settlement was directly measured by a linear variable differential transformer (LVDT) until the failures of the SC and SCP occurred. Afterwards, two multi-stage oedometer tests on the HKMC samples taken from the physical model were carried out after the load test to investigate its nonlinear compression behavior. The parameter values of clayey soils, SC and SCP are summarized and listed in Table 1. The oedometer tests and the load test on the SC and SCP can provide verified data for the HKMC, the SC, and the SCP.

Numerical Analyses and Parametric Study

Numerical Simulation of the Load Test

A numerical model was built to simulate the load test and to back-calculate the bearing capacities of the SC and the SCP (Ambily and Gandhi, 2007). The equivalent diameter was determined in the FE analysis, as presented in Figure 2(a). Axis-symmetric analysis was selected in the simulation. The horizontal displacements of the two sides were fixed. The top of the FE model is uniformly compressed. The drainage condition of the two sides is impermeable due to the symmetric of the model. The fine mesh was generated in the FE modelling, inducing total 1800 elements with a mesh size of 11.37 mm. The Mohr-Coulomb model was used for the SC and the SCP (Castro, 2017; Castro and Sagaseta 2009). The dilation angles were obtained from the relationship of $\psi = \phi_c - 30°$, where ϕ_c is the friction angle (Mohanty and Samanta, 2015), and the Poisson's ratio was taken as 0.2. The applied loading was consistent with the procedures in the physical model. As plotted in Figure 2(c), a good agreement between the analyzed results from the finite element and the physical model test data proves that the simulation domain and the values in Table 1 for the SC and the SCP are reasonable.

Numerical Simulation of the Physical Model

The consolidation process of the HKMC improved by the SC and the SCP was simulated based on the validated parameters of the physical model test. As illustrated in Figure 2(b), the equivalent diameter is the same as that used in the simulation of the load test. The uniform vertical loading of 40 kPa was applied on the top surface. A rigid plate was set on the top and bottom of the sand layer to simulate the equal strain condition in the physical model. Roller boundaries were set to ideally simulate the boundaries of the physical model (the side friction is neglected). Since strengthening by SCP and SC is mainly associated with the lateral expansion of the soft soil, the pile-soil interface was modeled by total adhesion contact rather than the interface element between the soft soil and columns. All the parameter values were listed in Table 1. In order to deeply understand the treated soft ground, different values of diameter, Young's modulus, friction angle of the columns and surcharge loading were applied in the FE modelling, as listed in Table 2.

Results and Discussions

Test Results under Vertical Loading of 40 kPa

Figures 2(d) and 2(e) show the variations of stress change on the columns and surrounding soft soil in the physical model. The stress variations from FE modelling are also calculated and compared. In the physical model test, the measured stresses are in the range of 250 kPa~326 kPa for the SC, while those of the SCP increase from 208 kPa to 277 kPa. Thus, the bearing capacity of the SC treated ground is higher than the SCP treated ground in the drained condition. In FE modelling, the stress variation shows a consistent trend. In the first 3 days, stresses on the SC increase from 208 kPa to 328 kPa and stresses on the SCP increase from 186 kPa to 265 kPa. For the stress change of surrounding soft soil, the measured stresses decrease from 45.4 kPa to 40.1 kPa for the SC treated soft soil and reduce from 49.9 kPa to 44.8 kPa for the SCP treated soft soil. In the FE analysis, the total vertical stress diminishes from 54 kPa to 49.5 kPa for the SC treated ground and decreases from 57 kPa to 49.8 kPa for the SCP treated ground within the first 3 days.

154 ***Numerical Results of Creep Settlement of the Soft Ground Improved by Columns***

155 The area replacement ratio is an important parameter in the treatment process of composite
156 foundation, which is defined as:

157 $$A_r = \frac{A_c}{A} = \frac{r_c^2}{r_e^2} \tag{3}$$

158 where A_c is the area of the column, r_c denotes the radius of the column, A is the total area, and r_e is
159 the equivalent radius of the area. The values of the area replacement ratio are calculated from Eq. (3)
160 based on the different values of r_c.

161 The creep effect of soft soil is usually neglected by setting a very small value of creep parameter ($\approx$
162 1% of the standard value, denoted as "no creep"). For the very small creep parameter value of soft soils
163 (termed as "no creep"), there is a stable force equilibrium after the consolidation:

164 $$\sigma_p A = \Delta\sigma_c A_c + \Delta\sigma_s \left(A - A_c\right) \tag{4}$$

165 Nevertheless, it is more realistic to consider the creep of the soft soils by setting the standard value of
166 creep parameter in soft soils. The stress on the top of soft soils gradually decreases because the creep
167 behavior of soft soils still occurs after consolidation. Then, the stress on the ground column increases
168 correspondingly based on the force equilibrium, expressed as:

169 $$\sigma_p A = \left(\Delta\sigma_c + d\sigma_c\right) A_c + \left(\Delta\sigma_s - d\sigma_s\right)\left(A - A_c\right) \tag{5}$$

170 where $d\sigma_s$ denotes the stress decrement of surrounding soft soil, $d\sigma_c$ is the stress increment on the
171 ground column. Substituting Eq. (3) into Eq. (4) and Eq. (5), we can get:

172 $$\frac{d\sigma_c}{d\sigma_s} = \frac{1 - A_r}{A_r} \tag{6}$$

173 It is found that the stress increment on the ground column due to the creep of surrounding soft soil would
174 decrease with the area replacement ratio. Thus, the higher value of the area replacement ratio is helpful
175 to reduce the creep influence on the stress concentration of the ground column.

176 Regarding the column-improved soft ground as one representative volume of mixture system (Shi
177 and Yin, 2017), there is a relationship between the total creep of mixture system and the creep of soft
178 soil (Shi and Herle, 2017):

179 $$\varepsilon_{creep} = \frac{\int_{V_s} \varepsilon(t) dV}{V_t} = \left(1 - A_r\right) \varepsilon_s(t) \tag{7}$$

180 where V_t and V_s are the volumes of the column-improved soft ground and surrounding soft soil,
181 respectively; $\varepsilon_s(t)$ is the creep behavior of the surrounding soft soil, which is related to the creep
182 parameter and stress-strain state (Yin and Graham, 1994):

183 $$\varepsilon_s(t) = \mu^* \ln\left(\frac{t + \Delta t_e}{t_0 + \Delta t_e}\right) \tag{8}$$

184 where Δt_e is the equivalent time related to the state of surrounding soft soil, μ^* is the creep coefficient
185 of untreated soft soil. When the soft soil is at the normally consolidated state, $\Delta t_e = 0$. By substituting
186 Eq. (8) into Eq. (7), a general creep settlement equation for the column-improved soft ground can be
187 obtained:

188 $$\varepsilon_{creep} = \left(1 - A_r\right) \mu^* \ln\left(\frac{t + \Delta t_e}{t_0 + \Delta t_e}\right) \tag{9}$$

189 As illustrated in Figure 3(b), the value of the equivalent time (Δt_e) is not only related to the amplitude
190 of the unloading stress but also dependent on the stress state before unloading. For A_r is 0.104, the stress
191 of surrounding soft soil decreases from 50 kPa to 40 kPa. For A_r is 0.416, the stress reduces from 25
192 kPa to 18 kPa. Although the unloading amplitude of A_r=0.104 is larger than that of A_r=0.416, it is
193 shown that the stress-strain state of A_r=0.416 is much closer than that of A_r=0.104 to the normal
194 compression line. In order to make a simplification, Eq. (9) can be expressed as:

195 $$\varepsilon_{creep} = \left(1 - A_r\right)^{\xi} \mu^* \ln\left(\frac{t}{t_0}\right) \tag{10}$$

where ξ is the reduction factor, which is related to stress decrement of the surrounding soft soil and the stress state. In this study, $\xi = 2.2\sin(\phi_c)$. The creep coefficient of the treated soft ground is regarded as: $\mu^*_{treated} = (1 - A_r)^{\xi}\,\mu^*$. Therefore, the creep improvement ratio is expressed as:

$$\beta_{creep} = \frac{1}{(1 - A_r)^{\xi}} \tag{11}$$

(a) The Influence of Young's modulus of column

As compared in the physical model, one main difference between SCs and SCPs is the value of Young's modulus. The range of Young's modulus of a stone column is usually between 25 MPa and 100 MPa (Castro, 2017). Taking the values of SCs and the SCPs as the reference, two other different values (12 MPa, 70 MPa) of Young's modulus in the FE modelling are utilized and compared. In Figure 4 (a), there is a good agreement between the calculated results of Eq. (11) and FE simulations with four different values of area replacement ratio (A_r). The creep improvement ratio nonlinearly increases with the area replacement ratio. Especially for the large value of the area replacement ratio, the creep settlement is largely reduced. In addition, it is observed that the creep settlement of treated soft ground is relatively independent of Young's modulus of columns, which is consistent with Sexton *et al.* (2017).

(b) The Influence of friction angle of column

The friction angle (ϕ_c) values of sand and stone materials are normally larger than 30°, thus, three different values of ϕ_c were investigated. The influence of friction angle of columns is shown in Figure 4 (b). It is found that the increase of ϕ_c could help to reduce the creep settlement of the column-treated soft ground, thus, the reduction factor ξ in Eq. (10) is related to the value of ϕ_c. As shown in Figure 4 (b), there is a good agreement between results of FE simulation and the calculated results from Eq. (11). Correspondingly, the influence of ϕ_c is correctly captured by Eq. (11).

(c) The Influence of surcharge loading

The influence of surcharge loading in the system of column-treated soft ground on the creep improvement ratio is presented in Figure 4 (c). Three different surcharge loadings from 40 to 160 kPa were studied since the surcharge loading of the composite foundation is normally within 200 kPa. It is shown that the surcharge loading has a slight effect on the creep improvement ratio. As explained by Sexton *et al.* (2017), the stress of soft soil could transfer to the columns before the columns are fully yielded. The calculated curves of Eq. (11) agree well with the results of the FE simulation with three different surcharge loadings.

Conclusions

In this study, a physical model test was conducted to compare the performance of the SC and SCP treated soft HKMC. FE modelling was utilized to analyze the stress variation of the SC and SCP, and the parametric study was performed to investigate the influences of column and surcharge loading on the creep settlement. The main findings and conclusions are drawn as follows:

a) According to the FE modelling under the loading of 40kPa, the *n*-values of the SC treated soft ground are in the range of 5.5~7.6, while the *n*-values range from 4.0 to 6.2 for the SCP improved soft soils.

b) The columns play the functions of replacing the soft soil and resisting the stress, which helps to reduce the creep settlement of the column reinforced soft ground. The reduction of creep settlement is an indicator of the safe long-term behavior of the soft soil reinforced by SC and SCP.

c) There are good agreements between the FE simulations and the calculated results from the proposed simplified equation for different Young's moduli, friction angles, and surcharge loadings.

Acknowledgements

The work in this paper is supported by grants (1-ZVCR. 1-ZVEH. 4-BCAU, 4-BCAW, 4-BCB1, 5-ZDAF) from The Hong Kong Polytechnic University, Hong Kong, China. We also acknowledge the supports by Research Institute for Sustainable Urban Development of The Hong Kong Polytechnic

241 University (PolyU), Center for Urban Geohazard and Mitigation of Faculty of Construction and
242 Environment of PolyU.

243 **Data Availability**

244 All data during the study are available in the submitted article and the detailed data values are available
245 from the corresponding author by request. And there is no model or generated code in this study.

246 **References**

247 Ambily, A. and Gandhi, S. R. (2007). Behavior of stone columns based on experimental and FEM analysis.
248 *Journal of Geotechnical and Geoenvironmental Engineering*, 133, 405-415.

249 Bouassida, M., and Carter, J. P. (2014). Optimization of design of column-reinforced foundations. *International*
250 *Journal of Geomechanics*, 14(6), 04014031.

251 BSI (British Standards Institution) (2016). Methods of Test for Soils for Civil Engineering Purposes. British
252 Standards Institute, Milton Keynes, BS:1377.

253 Castro, J., (2017). Modeling Stone Columns. *Materials*, 10(7), 782.

254 Castro J and Sagaseta C (2009). Consolidation around stone columns. Influence of column deformation.
255 *International Journal for Numerical and Analytical Methods in Geomechanics*, 33(7):851–877.

256 Feng, W. Q., Lalit, B., Yin, Z. Y., and Yin, J. H. (2017). Long-term Non-linear creep and swelling behavior of
257 Hong Kong marine deposits in oedometer condition. *Computers and Geotechnics*, 84, 1-15.

258 Han, J., and Ye, S. L. (2001). Simplified method for consolidation rate of stone column reinforced foundations.
259 *Journal of Geotechnical and Geoenvironmental Engineering*, 127(7), 597-603.

260 Kitazume, M. (2005). *The sand compaction pile method*, CRC Press.

261 Mohanty, P., and Samanta, M. (2015). Experimental and numerical studies on response of the stone column in
262 layered soil. *International Journal of Geosynthetics and Ground Engineering*, 1(3), 27.

263 Poorooshasb, H. B., and Meyerhof, G. G. (1997). Analysis of behavior of stone columns and lime columns.
264 *Computers and Geotechnics*, 20(1), 47-70.

265 Pugh, R. S. (2016). Settlement of floor slabs on stone columns in very soft clays. *Proceedings of the Institution*
266 *of Civil Engineers-Geotechnical Engineering*, 170(1), 16-26.

267 Sexton B.G. and McCabe B.A. (2016). Stone column effectiveness in soils with creep: a numerical study.
268 *Geomechanics and Geoengineering*. 11(4): 252–269.

269 Sexton, B. G., Sivakumar, V., and McCabe, B. A. (2017). Creep improvement factors for vibro-replacement
270 design. *Proceedings of the ICE - Ground Improvement*, 170(1), 35-56.

271 Shi, X. S., and Herle, I. (2017). Numerical simulation of lumpy soils using a hypoplastic model. *Acta Geotechnica*,
272 12(2), 349-363.

273 Shi, X. S., and Yin, J. (2017). Experimental and theoretical investigation on the compression behavior of sand-
274 marine clay mixtures within homogenization framework. *Computers and Geotechnics*, 90, 14-26.

275 Yin, J. H., and Graham, J. (1994). Equivalent times and one-dimensional elastic viscoplastic modelling of time-
276 dependent stress–strain behaviour of clays. *Canadian Geotechnical Journal*, 31(1), 42-52.

277 Yin, J. H., and Su, L. J. (2006). An innovative laboratory box for testing nail pull-out resistance in soil.
278 *Geotechnical Testing Journal*, 29(6), 451-461.

279 Yin, Z.-Y.; Karstunen, M.; Chang, C.S.; Koskinen, M. and Lojander, M. (2011). Modeling time-dependent
280 behavior of soft sensitive clay. *Journal of Geotechnical and Geoenvironmental Engineering*, 137(11): 1103-
281 1113.

282 Zhou, W. H., Yin, J. H., and Hong, C. Y. (2011). Finite element modelling of pullout testing on a soil nail in a
283 pullout box under different overburden and grouting pressures. *Canadian Geotechnical Journal*, 48(4), 557-
284 567.

285

286

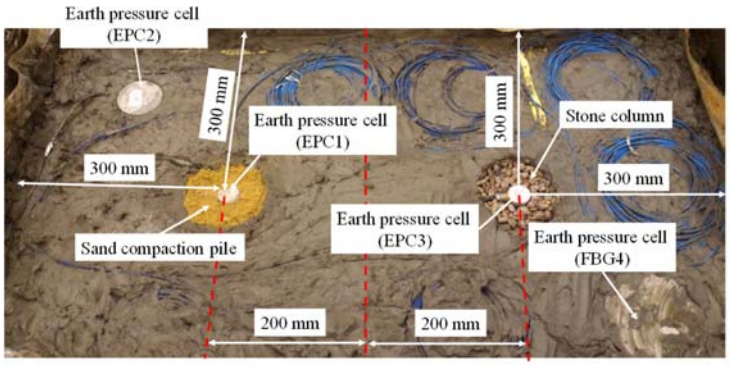

(a)

287

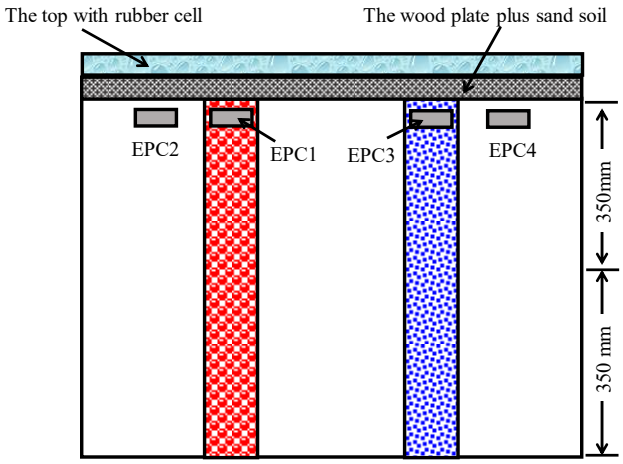

(b)

288
289

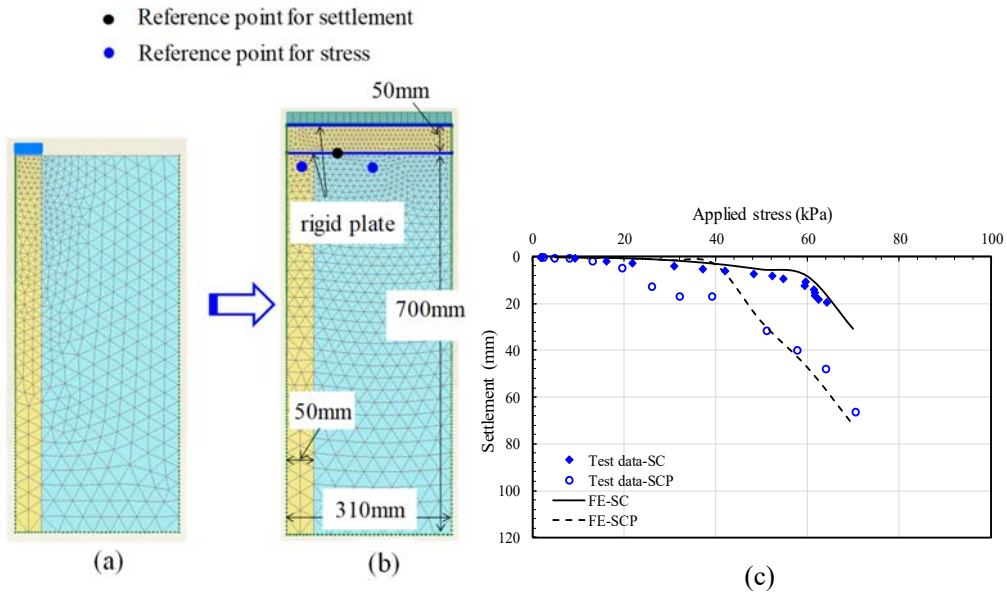
Reference point for settlement
Reference point for stress
50mm
rigid plate
700mm
50mm
310mm
(a)
(b)
Applied stress (kPa)
Settlement (mm)
Test data-SC
Test data-SCP
FE-SC
FE-SCP
(c)

290

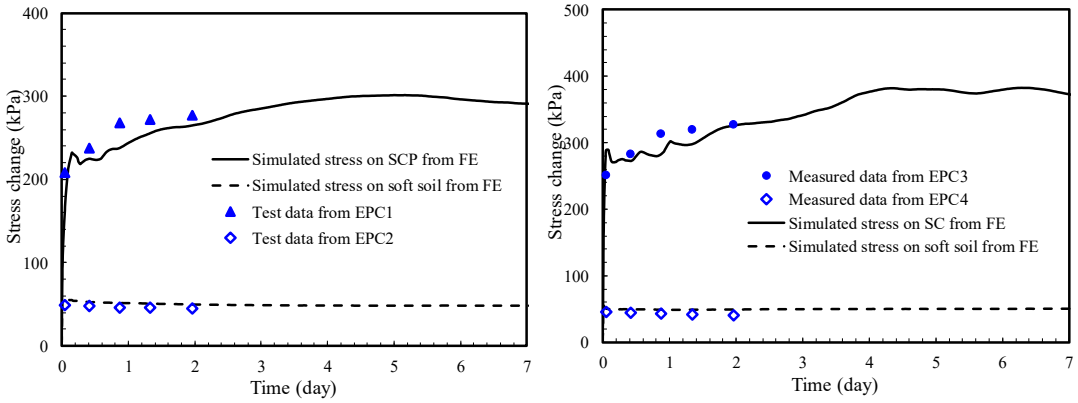
Stress change (kPa)
Time (day)
Simulated stress on SCP from FE
Simulated stress on soft soil from FE
Test data from EPC1
Test data from EPC2
(d)
Measured data from EPC3
Measured data from EPC4
Simulated stress on SC from FE
Simulated stress on soft soil from FE
(e)

291

292

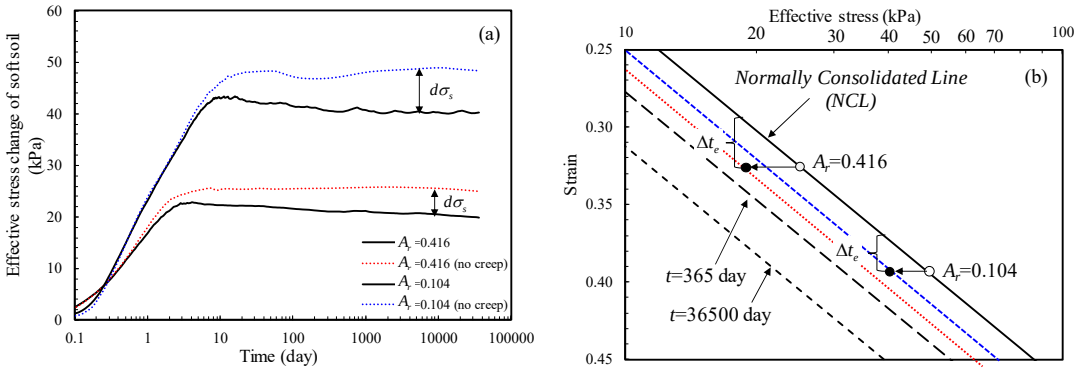
(a)
Effective stress change of soft soil (kPa)
Time (day)
$d\sigma_s$
$d\sigma_s$
A_r =0.416
A_r =0.416 (no creep)
A_r =0.104
A_r =0.104 (no creep)
(b)
Effective stress (kPa)
Strain
Normally Consolidated Line (NCL)
Δt_e
A_r=0.416
Δt_e
A_r=0.104
t=365 day
t=36500 day

293

294

295

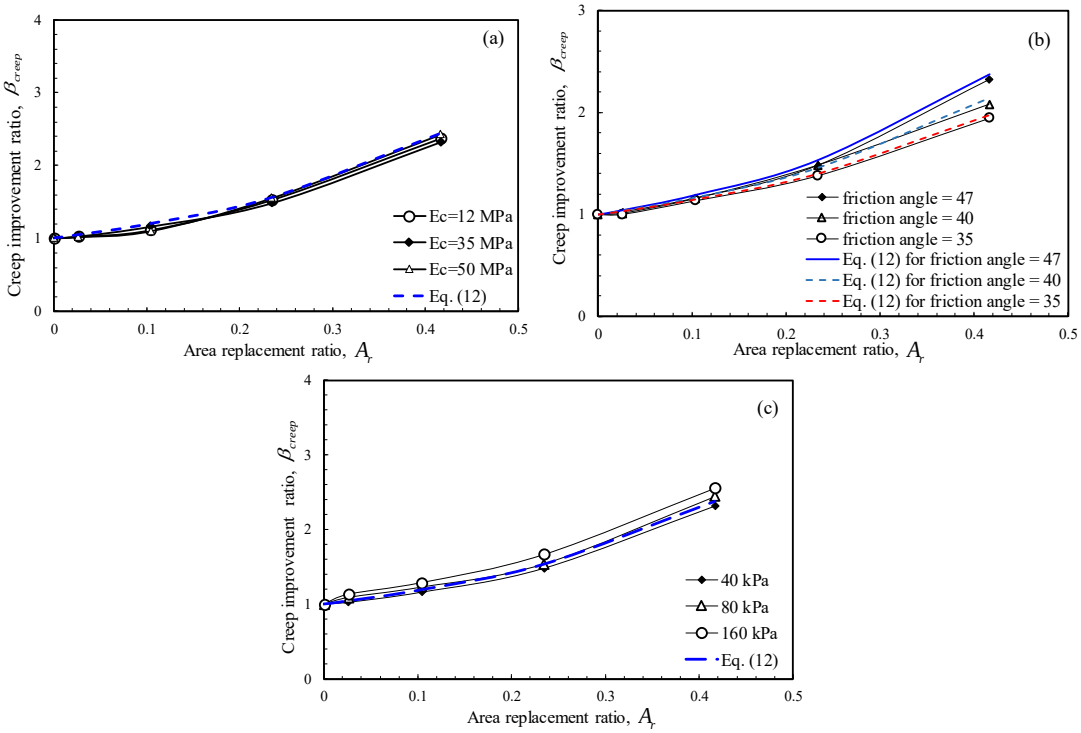

296

297

298

299 Table 1. Parameter values in the finite element simulations for the physical model test

Parameter (unit)	HKMD	SC	SCP
$\gamma_{soil}\ (kN/m^3)$	16	19	19
$k_x\ (m/day)$	3.5×10^{-4}	1.0×10^{-1}	1.0×10^{-1}
$k_y\ (m/day)$	3.5×10^{-4}	1.0×10^{-1}	1.0×10^{-1}
$c^{'}\ (kPa)$	0.1	0.1	0.1
$\phi^{'}\ (°)$	30	47	42
ψ	-	17	12
POP (*kPa*)	10		
κ^{*}	0.026	-	-
λ^{*}	0.101	-	-
μ^{*}	0.0076	-	-
v	0.15	0.2	0.25
$E_c\ (kN/m^2)$	-	35250	12000

300

301

302 Table 2. Parametric analysis of column in the finite element simulations

Column Radius	Variable				Constant			
r_c (mm)	E_c (kN/m^2)	ϕ_c (°)	ψ (°)	σ'_v (kPa)	γ_c (kN/m^3)	v	c' (kPa)	$k_x = k_y$ (m/day)
50, 100, 150, 200	12000	47	17	40	19	0.2	0.1	0.1
50, 100, 150, 200	35250							
50, 100, 150, 200	50000							
50, 100, 150, 200	35250	47	17	40				
50, 100, 150, 200		40	10					
50, 100, 150, 200		35	5					
50, 100, 150, 200	35250	47	17	40				
50, 100, 150, 200				80				
50, 100, 150, 200				160				

303

304